Article

Ultrasensitive Photoelectrochemical Biosensing of Cell Surface N-glycan Expression Based on the Enhancement of Nanogold-assembled Mesoporous Silica Amplified by Graphene Quantum Dots and Hybridization Chain Reaction

Shenguang Ge, Feifei Lan, Linlin Liang, Na Ren, Li Li, Haiyun Liu, Mei Yan, and Jinghua Yu

ACS Appl. Mater. Interfaces, **Just Accepted Manuscript** • DOI: 10.1021/acsami.6b11966 • Publication Date (Web): 08 Feb 2017

Ultrasensitive Photoelectrochemical Biosensing of Cell Surface N-glycan Expression Based on the Enhancement of Nanogold-assembled Mesoporous Silica Amplified by Graphene Quantum Dots and Hybridization Chain Reaction

Shenguang Ge,[†,§] Feifei Lan,[†,§] Linlin Liang,[†] Na Ren,[‡] Li Li,[†] Haiyun Liu,[†] Mei Yan,[†] Jinghua Yu[†,*]

[†]School of Chemistry and Chemical Engineering, University of Jinan, Jinan 250022, P. R. China.

[‡]School of Biological Science and Technology, University of Jinan, Jinan 250022, P.R. China.

[§]These authors contributed equallly to this work.

*Corresponding author: Jinghua Yu

E-mail: ujn.yujh@gmail.com

Telephone: +86-531-82767161

ABSTRACT: An ultrasensitive photoelectrochemical (PEC) biosensor for N-glycan expression based on the enhancement of nanogold-assembled mesoporous silica nanoparticles (GMSNs) was fabricated, which also combined with multibranched hybridization chain reaction (mHCR) and graphene quantum dots (GQDs). In this work, the localized surface plasmon resonance, mHCR and GQDs-induced signal amplification strategies were integrated exquisitely and applied sufficiently. In the fabrication, after porous ZnO spheres, immobilized on the Au nanorod-modified paper working electrode, were sensitized by CdTe QDs, the GMSNs were assembled on the CdTe QDs. Then the photocurrent efficiency was improved by the sensitization of the CdTe QDs and the localized surface plasmon resonance of GMSNs. Successively, the products of mHCR with multiple biotins for multiple horseradish peroxidase binding and multiple branched arms for capturing the target cells were attached on the as-prepared electrode. The CL emission with the aid of horseradish peroxidase was served as an inner light source to excite photoactive materials for simplifying the instrument. Furthermore, the aptamer could capture the cancer cells by highly efficient cell recognition ability, which avoided the conventional routing cell counting procedures. Meanwhile, the GQDs served as signal amplication strategy was exerted in the process of N-glycan evaluation due to competitive absorption of exciting light and consumption of H_2O_2 served as the electron donor of the PEC system and the oxidant of luminol-based CL system. This judiciously engineered biosensor offered an aussichtsreich platform for the exploration of N-glycan-based physiological processes.

KEYWORDS: Photoelectrochemical, Microfluidic paper-based analytical device, Localized surface plasmon resonance, Multibranched hybridization chain reaction, N-glycan evaluation

1. INTRODUCTION

Glycosylation, one major protein modification in eukaryotes, plays crucial role in majority of biological processes.[1,2] As is well-known to all, N-glycosylation can regulate the protein trafficking and folding. In addition, the glycan of N-linked glycosylation (N-glycan) attached to the side chain of asparagines participate in the biomolecule interactions, thus they can mediate a good deal of physiological and biological events such as tumor progression.[3-5] Glycan epitopes served as surface markers can recognize and detect different kinds tumor.[6] The glycan expression on cell membranes, a dynamic process related to the cellular condition and status, can reflect the pathophysiological steps of the morbid state.[7] Aberrant N-glycan not only involve in many pathological phenomena, but also is hallmark of many diseases, such as Alzheimer's disease,[8] cancer,[9] and infectious diseases.[10] As a consequence, the cell surface N-glycan evaluation is primarily pregnant for deciphering roles in disease development and clinical diagnostics and therapeutics.

Currently many well-established methods about glycomics analysis have been reported, for instance, mass spectrometry,[11] capillary electrophoresis,[12] nuclear magnetic resonance,[13] and high-performance liquid chromatography.[14] Although these methods can reveal the structural details superiorly, many severe drawbacks are also distinct. The infrastructures applied in these analytical methods are normally pricy as well as sophisticated, and the procedures are time-consuming and destructive, which limit the widespread clinical practice to a great extent.[15,52] To make up for the deficiency, there is a urgent need to develop a method with potential applications of simple, rapid, inexpensive, robust for dynamic analysis of glycan on cell surfaces.

Paper-based microfluidic systems[16-18] have been widely used as a platform for biological assay in recent years to satisfy the growing need for simple, cost-effective, point-of-care diagnostic devices. Paper possesses high specific surface area on account of its high surface roughness and internal porosity.[18] Besides it is also inexpensive, flexible, easily shaped by cutting or folding, and disposable by

incineration.[20] Up to now, the paper-based photoelectrochemical (PEC) sensors have had a wide range of applications in the analysis for polytype testing sample.[21-23] However, fewer reports about paper-based PEC sensors that used for simultaneously dynamic analysis of N-glycan presented on the cell surface and cytosensing are reported. In traditional PEC analysis, under the action of excitation light, the photoinduced electrons from the photoelectric material take part in the process of transfer. The adverse background signal was decreased on account of the separation of the light (excitation source) and current (detection signal).[24-26] Meanwhile, the apparatus offered physical light source make the the process of detection for analytes is cumbersome, which also violate the concept of instrument miniaturization. Therefore, chemiluminescent (CL) emission was introduced in order to avoid the external physical excitation light source inspired by the inner light source for PEC.[27] Furthermore, to realize PEC detection, light emission with different wavelengths can be obtained by changing the experimental condition of the luminol-based CL system.[28,29] As we all known, hydroxyl radical was producted from H_2O_2 by the catalysis of the horseradish peroxidase (HRP), which further catalyzed the CL reaction of luminal with enhanced CL signal.[30,31] Thus, this reaction was applied to our strategy for offering the internal excited light source. To achieve highly sensitive detection on the PEC biosensor, enhanced photocurrent intensity and signal amplification strategies are necessary. In order to enhance the photocurrent intensity, cosensitized structure, localized surface plasmon resonance (LSPR) and multibranched hybridization chain reaction [32,33](mHCR) were brought into our system. ZnO-based semiconductor materials are very attractive and promising photoactive material due to their low cost, excellent biocompatibility, eminent chemical and thermal stability.[34,35] For the suitable band gap of ZnO and CdTe quantum dots (QDs), the transfer process of electron excited from the CdTe QDs to ZnO can take place readily, which could not only effectively enhance the utilization of light energy but also reduce the electron-hole recombination.[36] Recently, the LSPR-mediated control over the emission property has become a hotspot. LSPR, arised from the collective oscillation of conduction electrons of metal nanostructures, can excite high-energy

electrons emerging on metal surface,[37] which bring the noble metal nanoparticles several unique properties, such as the unique plasmon absorbance features, intensive localized electric field in the vicinity and visible light-induced charge separation.[38] In the case of plasmonic metallic nanostructures coupled to other substrates, the electrons excited from the metal could be deliveried in the conduction band of the semiconductors materials via surmounting the Schottky barrier.[39-42] In the proposed biosensor, the energetic electrons from the surface plasmons of the Au NPs were injected into the conduction band of the semiconductor material (CdTe QDs), then rapidly passed on to the electrode through porous ZnO. Metallic nanoparticles, especially nanogold (Au NPs), were widely applied due to their strong LSPR, high extinction coefficient and broad absorption spectra.[43] What's more, the mesoporous silica nanoparticles (MSNs) with large surface-to-volume ratios and uniform pore diameters were induced for loading plenty of Au NPs, which significantly enhanced the LSPR absorption efficiency (nanogold assembled the MSNs was defined as GMSNs). In addition, simple but effective signal amplification was achieved by graphene quantum dots (GQDs) because of the distinct optical and electronic natures. On account of quantum confinement effect and quantum size effect, the bandgap is about 2.0 ev. Besides, the properties of excellent biocompatibility and unique solubility have made GQDs attract increasing attention.[44-46]

Herein, we present a novel PEC biosensor. Experimentally, porous ZnO spheres were covered on the paper working electrode with Au nanorod (Au-PWE), then the CdTe QDs and GMSNs were attached to the as-prepared electrode successively. The horseradish peroxidase (HRP) labled double helices of DNA with multiple branched arms (HRP-mdhDNA) with carboxyl was linked on the ethanediamine treated GMSNs via the formation of amide bond, which could make the luminol-based CL system offer lignt source for the biosensor. Under the inner light source, the porous ZnO sensitized by CdTe QDs produced high photocurrent response at the aid of the the localized surface plasmo resonance of GMSNs. The ingenious project that certain multiple branched arms were designed as the aptamper of the MCF-7 cells enabled

the target cells to be captured on the surface of the as-obtained electrode by the specific recognition reaction between the MCF-7 cells and the aptamers. The photocurrent response decreased with the increasement of the target cells due to the large steric hindrance. Meanwhile, concanavalin A (Con A) conjugated GQDs was applied in this system for the detection of N-glycan presented on cell surface due to the unique PEC properties of GQDs. The GQDs connected to the cells would competitively absorb the CL and consume the electron donor of the PEC system, resulting in evidently weakened photocurrent intensity. N-glycan Expression on cell membranes plays a crucial role in the specific recognation between the Con A and target cells. Thus, the GQDs attached Con A could reflect the N-glycan Expression indirectly by the change of the photocurrent intensity. The designed PEC biosensor opened a new era for sensitive evaluate the expression of N-glycan on the cell surface and offered a promising platform for clinical diagnostics and drug screening.

2. EXPERIMENTAL SECTION

2.1. Synthesis of Porous ZnO Spheres. Porous ZnO spheres was obtained according to the previous work with appropriate modifications.[47] The details are presented in the Supporting Information.

2.2. Preparation of the GQDs and CdTe-NH_2 QDs. The GQDs were produced by a chemical oxidation approach and the CdTe-NH_2 solution was synthesized according to the previous work,[48,49] the details was seen in the Supporting Information.

2.3. Synthesis of GMSNs. The utilized GMSNs was fabricated according the previous report,[50] and the synthesis details was shown in Supporting Information.

2.4. Preparation of the PEC Detection Areas. The manufacturing process of the proposed PEC biosensor was showed in Scheme 1. After the porous ZnO was immobilized on the surface of the Au-PWE, GMSNs were linked on the CdTe QDs modified ZnO/Au-PWE. Then the HRP-mdhDNA was attached onto the as-obtained electrode. Followed that the target cells and the expression of the N-glycan presented on the cell surface could be evaluated. The details of fabrication process for

biosensors were offered in the Supporting Information.

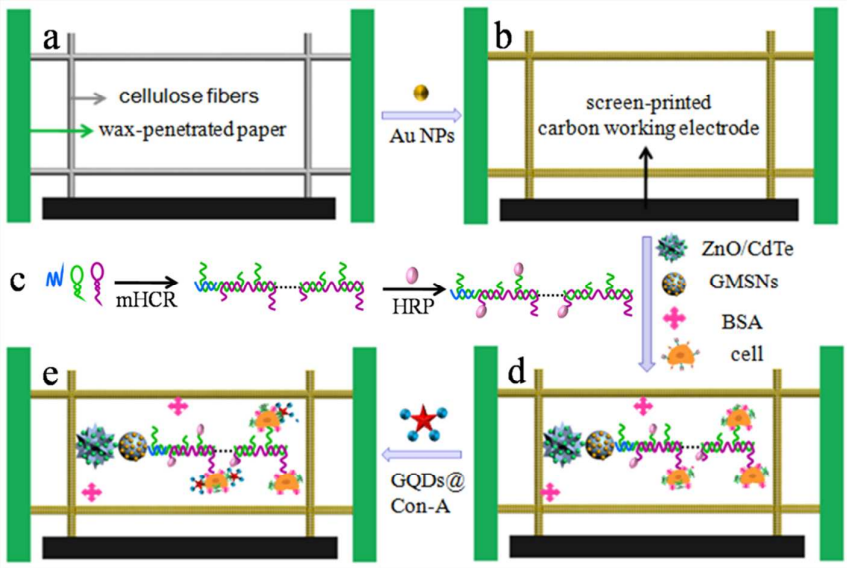

Scheme 1. Schematic diagram of the manufacture procedures for the PEC detection area. a: The cellulose fibers was printed with wax, and the unprinted cellulose was serverd as work zone. b: The Au NPs was grown on the hydrophilic work zone. c: HRP was bounded on the mdhDNA formed by the multibranched hybridization chain reaction. d: The ZnO, CdTe, GMSNs, HRP-mdhDNA were modified on the Au-PWE in sequence, then the target cell was recongnized by the mdhDNA contained the aptamer . e: The GQDs@Con-A linked on the captured target cell, which came true the signal amplication of the system.

3. RESULTS AND DISCUSSION

3.1. Characterization of Au-PWE and porous ZnO. As can be seen in the Figure 1A, the paper served as working electrode owned many macropores and rough surface, which offered an unique attachment microenvironment for the Au nanorod seed. A pyknotic layer of Au nanorod was obtained on the cellulose fibers of paper work zone (Figure 1B), and magnified scanning electron microscopy (SEM) images was shown in Figure 1C. The Au nanorod with high conductivity not only strengthened the conductivity of the paper work electrode but also offered active surface for ZnO, then the 4-aminothiophenol functioned ZnO could anchored the Au-PWE. The X-ray

diffraction (XRD) patterns of bare paper and Au-PWE were shown in Figure 1D. Three distinguishing diffraction peaks at 38.36, 44.54 and 64.75 were observed in the XRD pattern of Au-PWE (curve b) compared with that of bare paper (curve a), which corresponded to the (111), (200) and (220) crystallographic planes of cubic respectively (JCPDS card No 004-0784). Figure 1D certified that Au nanorod had been successfully generated on paper. The SEM images (Figure 1E) and TEM image (Figure 1F) showed that the product possessed porous structures and the average size was about 300 nm. In additon, the porous structure made ZnO provide high ratio of surface area to weight for the attachment of CdTe QDs, which would greatly improve the photocurrent response of the proposed biosensor. The diffraction peaks in Figure S1 could be assigned to (100), (002), (101), (102), (110), (103), (200), (112), (201) planes of hexagonal phase ZnO, which verified the successful synthesis of ZnO because the diffraction peaks were well consistent with the value in the standard card (JCPDS 89-7102).

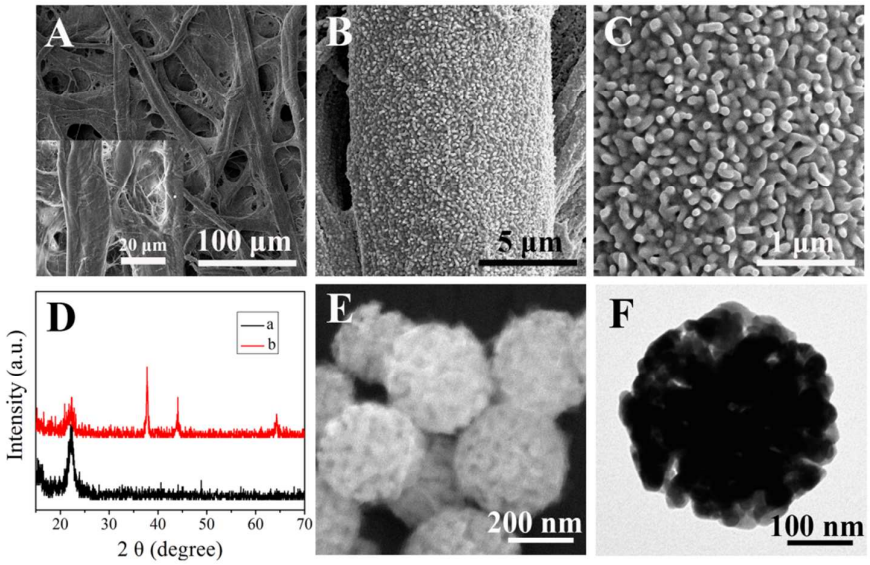

Figure 1. (A) SEM images of bare PWE; Inset: magnified SEM images of bare PWE; (B) SEM images of Au-PWE; (C) magnification of (B);(D) XRD patterns of the (a) bare paper, (b) Au-PWE; SEM image (E) and TEM image (F) of porous ZnO.

3.2. Characterization of MSNs and GMSNs. Figure 2A shows the SEM image of the synthesized MSNs, which indicated a type of spherical morphology with the average size of 80 nm. As could be seen from the Figure 2B, the three-dimensional network of MSNs could be obviously observed, which could provide the large surface for the growth of Au NPs. After the assembly of Au NPs, the pore size decreased and the network of GMSNs (Figure 2C) displayed more indistinct than unmodified MSNs, which could further confirm the in situ growth of Au NPs on the surface of MSNs.

3.3. Characterization of GQDs and CdTe QDs. GQDs possess mangy distinct properties, especially in optical and electronic area, and it can be seen from Figure 2D. With the increase of the excitation wavelength, the mission wavelength exhibited a slightly red shift, which might be resulted from the reason of GQDs' different emissive sites.[44] As can be seen from the UV-vis absorption spectrum, the GQDs had a obvious peak at 228 nm and possessed a broad absorption below the wavelength of 600 nm, which were accordant with the previous work.[48] The GQDs had a average diameters of about 8 nm seen from in Figure S2A. The GQDs were characterized by X-Ray photoelectron spectroscopy (XPS) and Fourier transform infrared (FT-IR) spectroscopy (Figure 2E, Figure S2B) in order to research the surface groups. We can seen from the XPS that the GQDs mainly presented three kinds of carbons, oxygenated carbon, graphitic carbon as well as nitrogenated carbon. The existence of nitrogen resulted from the oxidation of HNO_3 in the synthesis of GQDs (Figure 2E, F). In the FT-IR spectra (Figure S2B), the GQDs had characteristic peaks at 3428 cm^{-1}, 1382 cm^{-1} and 1085 cm^{-1}, which respectively corresponded to the O-H group stretching, C-O group deformation and the C-OH group stretching. The above results certified the as-synthesized products possessed -OH and -COOH groups.

As can been seen in Figure S2C, the diameter of the as-obtained CdTe QDs was about to be 2.6 nm, which were consistent with the obtained result accroding to Peng's empirical equations: $D=(9.8127\times10^{-7})\lambda^3-(1.7147\times10^{-3})\lambda^2+1.0064\lambda-194.84$.[51] According to the UV-vis spectral (Figure S2D), the CdTe QDs exhibited an absorption range below 545 nm and the absorbance peak (curve a) appeared at 495 nm. The

CdTe QDs served as sensitizer was anchored on the porous ZnO, which made the cosensitized structure consist of the large band gap photoelectric material and one small bandgap sensitizer. Different semiconductors own different optimal absorption ranges due to their different band gaps. The produced cosensitized structure with cascade band-edge levels cannot only adequately utilize the light energy but also effectively promote charge separation and consequently enhance the photocurrent conversion efficiency. As can be seen the inset part in Figure S2D, the photocurrent response of CdTe/ZnO/Au-PWE had an obvious increasement compared with that of ZnO/Au-PWE. The results proved that the sensitization of the CdTe QDs made ZnO have the better photoelectric property.

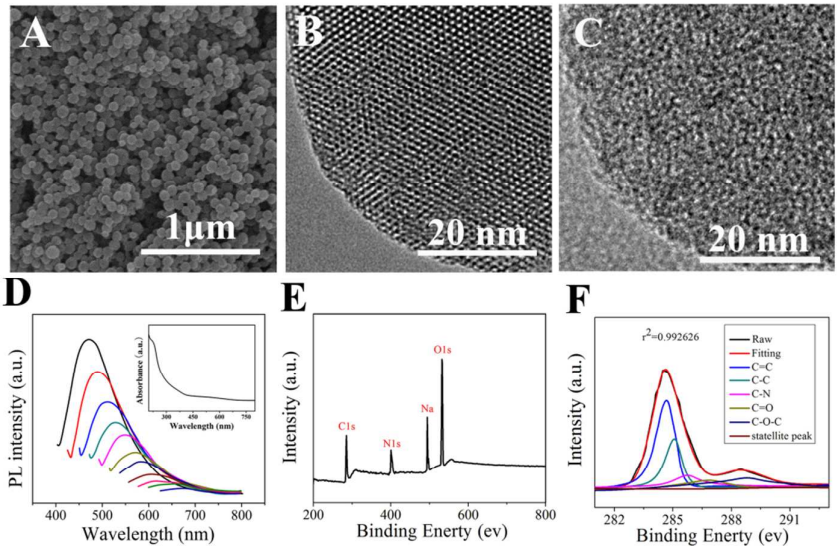

Figure 2. SEM image (A) and HRTEM image (B) of the MSNs; (C) magnified HRTEM image of GMSNs; (D) PL emission spectra of GQDs (inset: UV-vis absorption spectra); (E) XPS analysis surveys of GQDs; (F) XPS C 1s analysis of GQDs.

3.4. PEC Behaviors of the Biosensor. In order to test the fabrication of the biosensor, PEC measurements of process with different states were recorded. The mdhDNA produced from mHCR could provide large multiple branched arms for multivalent binding of HRP and serving as the aptamer of the MCF-7 cells, which offered superior CL conditions for producing sufficient light source for the PEC biosensor and

afforded a platform for the capture of the target cells via the aptamper in the mdhDNA. As shown in Figure S3A, the luminol-HRP-H_2O_2 CL system presented an excellent CL response. The analysis results of the electrodes with different states were shown in Figure 3A, which were carried out in the solution contained H_2O_2 and luminol. Before anchored the biosensor with HRP-mdhDNA, a negligible photocurrent (curve a) was obtained, which ascribed to little light emission produced without the catalysis of HRP. However, HRP-mdhDNA introduced into the biosensor triggered the reaction of luminol-HRP-H_2O_2, which brought light source for the PEC system. A strong photocurrent response was obtained (curve b), which indicated the feasibility of the CL served the light source in this biosensor. Light induction would trigger the generation of LSPR of GMSNs then promoted electron transfer, which made the PEC sensors produce an obvious photocurrent response. The contrast test was shown in Fig. S3B，the pure ZnO almost had no photocurrent signals in our system (curve a), and the CdTe QDs generated a photocurrent (curve b) with about 188 nA. Interestingly, the porous ZnO modied with CdTe QDs had a obvious increase compared with bare

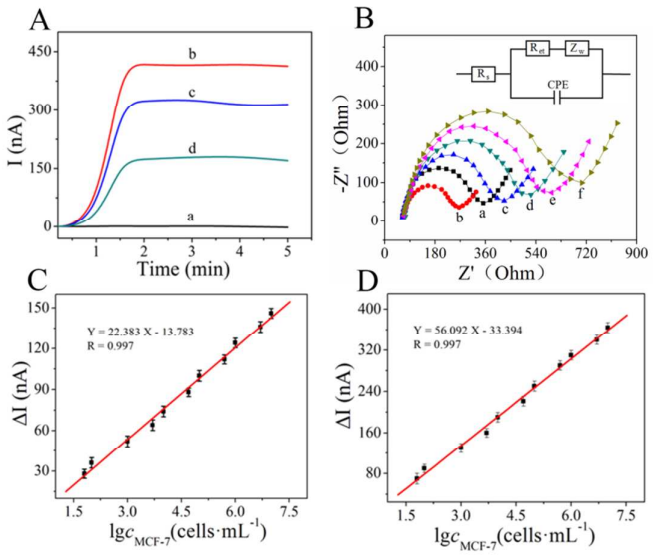

Figure 3. (A) the photocurrent responses of GMSNs/CdTe/ZnO/Au-PWE electrodes (a) before and after (b) anchored HRP-mdhDNA, (c) incubated with MCF-7 cells (1.0×10^5 cells mL^{-1}), (d) after further incubated GQDs@Con A; (B) EIS of (a) bare PWE, (b) Au-PWE, (c) ZnO/Au-PWE, (d) CdTe/ZnO/Au-PWE, (e) after anchoring GMSNs, (f) after further linking with HRP-mdhDNA;

Inset: the electrical equivalent circuit applied to fit theimpedance data; Rs, Rct, Zw, and CPE represent the Ohmic resistanceof the electrolyte, charge-transfer resistance, Warburg impedance, andconstant phase angle element, respectively. (C) Logarithmic calibration curve for cells ($\Delta I=I_0 - I_1$); (D) Logarithmic calibration curve for cells attached GQDs ($\Delta I=I_0-I_2$). I_0, I_1 and I_2 are the photocurrent of the HRP-mdhDNA /GMSNs/CdTe/ZnO/Au-PWE, after incubation with cells and further incubation with GQDs.

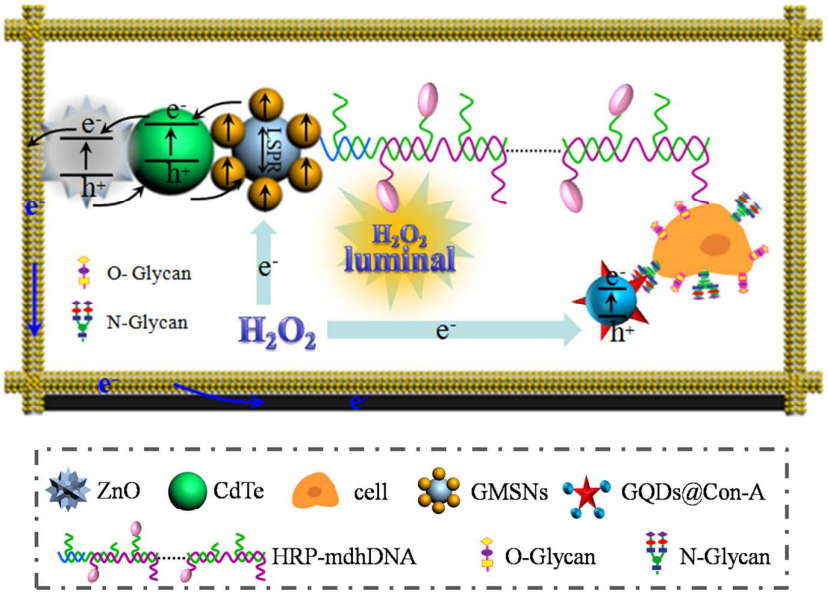

Scheme 2. Schematic representation of the PEC analytical principle.

ZnO with a photocurrent responses of 345 nA (curve c). The mere MSNs could not enhance the photocurrent response and even have inhibitory effect on the CdTe/ZnO/Au-PWE（curve d, decreased to 237 nA). In additon, the photocurrent responses further increased after modified with GMSNs (curve e), which ascribed the LSPR of the GMSNs. After the capture of target cells, the electrodes were further cultivated in the solution with GQDs@Con A nanoprobes. The photocurrent intensity

dramatically decrease (curves c and d) mainly ascribed to two reasons. On the one hand, the huge steric effect of cells and GQDs@Con A hindered the holes's cavenging. On the other hand, GQDs competitively absorbed the CL served as the internal excited light source and consumed the electron donor of the PEC system. The

mechanism of biosensing was shown in Scheme 2.

Electrochemical impedance spectroscopy (EIS), an effective tool to characterize interface performance of the electrodes,[52] was applied to further study the stepwise assembly process of the biosensor (Figure 3B). The electron-transfer resistance (*Ret*) of Au-PWE had a obvious decrease compared with the bare PWE (curve a), which attributed to the excellent electrical conductivity of the Au nanorod. After the porous ZnO was coated onto Au-PWE, remarkably increased EIS (curve c) certified that the successful assembly of photoelectric material, ZnO, which made the redox probe untoward to close to the surface of electrode. Subsequently, the *Ret* increased sequentially (curves d-f) when CdTe, GMSNs, HRP-mdhDNA were introduced on the surface of the Au-PWE, testifying that the assembly of different substances inhibited the transmission of electrons. To further improve the sensitivity of biosensor, mHCR reaction was employed to produce long products with multiple biotins for HRP to furnish the sufficient light source and multiple branched arms (aptamer of MCF-7 cells) to recognize cell. The products of mHCR were proved by electrophoretic analysis and AFM images (Figures S4Aand S4B). The gradually increased *Ret* testified the the PEC biosensor had been constructed successfully.

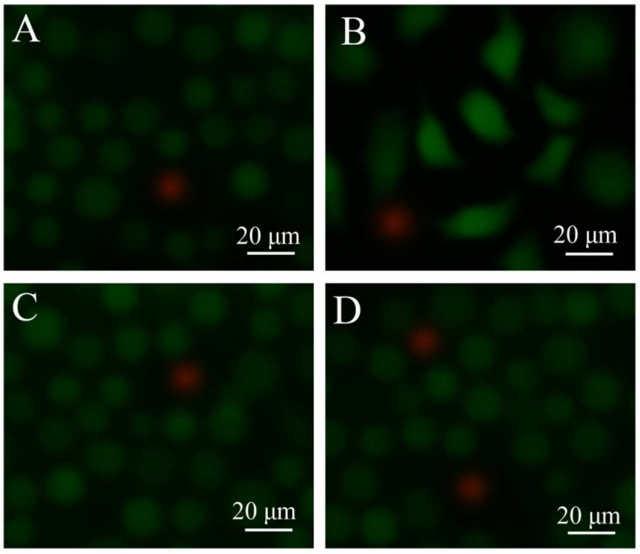

Figure 4. Fluorescence microscopy imaging of the MCF-7 cells stained after the incubation with GQD_S in the culture dish for 1 h (A) and 10 h (B); Fluorescence microscopy imaging of the MCF-7 cells captured on the prepared electrode for 1 h (C) and 3 h (D). (green fluorescence: living cells; red fluorescence: dead cells.)

To inspect the cellular ability, a standard staining tests were carried out with the assistance of Calcein AM and propidium iodide. Interestingly, the results in Figure 4 showed that the cell viability was about 96%. Figure 4A and B exhibited fluorescence microscopy image of stained MCF-7 cells after incubation with GQD_S for 1 h and 10 h, respectively. The MCF-7 cells presented a well living morphology, which indicated the GQDs had low cytotoxicity to the target cells. After the incubation of 10 h (Figure 4B), plenty of fusiform cells was observed with few dead cells, manifesting the as-prepared biosensor had excellent biocompatibility. The fluorescence microscopy images of the captured MCF-7 cells with the incubation of 1 h and 3 h (Figure 4C, D) were showed to investigate the viability of captured cells. In the fluorescence microscopy imaging, the vast majority of cells presented the luorescence Calcein AM (green fluorescence signals), which demonstrated the most of target cells still alive in the process of bioanalysis.

3.5. Cytosensing of the Biosensor. Under optimal conditions (Figure S5), the change of photocurrent intensity (ΔI) of the biosensor for MCF-7 cells with different concentrations was shown in Figure 3C. The photocurrent signal reduced regularly and the ΔI of the biosensor increased correspondingly. A good linear relationship was obtained in the range of 100 to 10^7 cells per mL. The equation of the calibration curve was ΔI=22.383x-13.783logc_{cell} (cells mL^{-1}), and the correlation coefficient was 0.997. The detection limit was estimated to be 33 cells per mL at 3σ. Furthermore, when the proposed biosensor captured cells was incubated with GQDs@Con-A nanoprobes, GQDs were loaded onto the surface of the cancer cells to competitively absorb the CL served as excitation source and consume the H_2O_2. Besides the increased steric hindered the electron transfer, leading to gradually reduced photocurrent intensity and increased ΔI of the biosensor. A similar linear relationship between the ΔI of the

biosensor and the logarithm of the concentration of MCF-7 cells incubated with GQDs was obtained (Figure 3D). The ΔI was proportional to the logarithmic value of MCF-7 cells in the range from 63 to 10^7cells per mL. The equation of the calibration curve with the limit of detection of 21 cells mL^{-1} was ΔI=56.092x-33.394 logc_{cell} (cells mL^{-1}), and the correlation coefficient was 0.997. The broad detection range, low detection limit (Table 1) and high sensitivity could be ascribed to the multivalent effect of the aptamer that we had reported.[53,54] The facts demonstrated that PEC signal of the proposed biosensor could be applied for sensitive cell detection and N-glycan expression profiling.

Meanwhile, the resulting biosensor exhibited high specificity and stability (Figure S6). Specificity was a key factor for the designed biosensor, since the nonspecific adsorption can influence the accuracy of the detection results. As shown in Figure S6A, there were remarkable ΔI when the electrode was immersed in the MCF-7 cells solution. Minor ΔI were observed in the solution with K562, A549, and Hela cells, which gave small interference to the prepared biosensor. Furthermore, the ΔI of the biosensors incubated in the solution MCF-7 + K562, MCF-7 + A549, MCF-7 + Hela., MCF-7 + K562 + A549 + Hela were a little difference (less 8 %) compared with the ΔI of the biosensors incubated in the solution only contained MCF-7 cells, which was comparable with that the interference with less 10 % at the previous PEC biosensor for HL-60 cell line.[61] The results suggested that the as designed PEC biosensor possessed excellent selectivity to MCF-7 cells. In additon, stability of the biosensor was also an effective criterion in application. The ΔI decreased gradually with the storage time increased from 5 to 30 days. However, no detectable loss of the initial response was observed for different storage times. After 30 days of storage, the PEC biosensor reserved about 89.96 % of its original response implying the good storage stability, which was comparable with our previous work.[6062]

Table 1. Comparison of biosensors for cancer cell detection by various methods.

Method[a]	Cells	Linear range (cell mL^{-1})	Detection Limit (cell mL^{-1})	References
EC	SMMC-7721	500-1.0×10^6	500	55
PL	MCF-7	500-1.0×10^5	500	56
CL	HCCC-9810	600-1.0×10^7	300	57
ECL	CCRF-CEM	100-1.0×10^5	38	58
FL	MCF-7	100-1.0×10^7	33	59
PEC	SMMC-7721	5000-1.0×10^7	5000	60
PEC	MCF-7	63-1.0×10^7	21	This work

[a] EC: Electrochemistry; PL:Photoluminescence.; CL: Chemiluminescence; ECL: Electrogenerated chemiluminescence; FL: Fluorescence; PEC: Photoelectrochemistry.

3.6. Evaluating Cell Surface N-glycan Expression. N-glycan is extraordinary important in the communications between cells as well as cell-matrix interactions. In this proposed biosensor, the ΔI of the biosensor attached GQDs resulted from both cell concentration and N-glycan expression. Cells captured on the electrode surface resulted in a sharp decrease because the huge steric effect impeded the holes's cavenging. Thus the process of cell counting would be avoided, which eliminated the artificial errors in a complex biological matrix. In addtion, the N-glycan expression on the cell surface can be measured by the ΔI of biosensors with different states. The N-glycan expression of MCF-7 cells was analyzed with the proposed biosensor under the treatment of tunicamycin (TM), benzyl 2-acetamido-2-deoxy-α-D-galactopyranoside (BG) and peptide-N-glycosidase F (PNGase F). TM and BG can suppress the expression of N-glycan and O-glycan respectively. PNGase F can make the N-glycan shed from asparagines by the effect of enzymatic cleavage. The cells without treated served as the control test. As shown in Figure S7, compared with the contrast test, the ΔI of TM treated cells decreased to 56.86% for 48 h treatment, which was because TM had a tremendous hindrance function on the biosynthesis of N-glycan and could further inhibit the N-glycan expression. However, BG-treated cells had little or no changes because BG could

suppress O-glycosylation but not interfere with N-glycosylation.[6163] In comparation with the control test, the ΔI of NGase F-treated MCF-7 cells reduced to 42.16%, which had a same level compared with the effect of TM-treated MCF-7 cells. It was demonstrated that the proposed biosensor could dynamically evaluate cell surface N-glycan expression with high sensitivity.

4. CONCLUSION

In summary, an ultrasensitive paper-based biosensor for MCF-7 cells and in situ evaluation of cell surface N-glycan expression has been developed by combining the signal amplication of the GQDs@Con A nanoprobe and the specific binding of aptamer in mdhDNA and Con A to the target cells. What's more, the detecton for cells and N-glycan expression on cell surface could be simultaneously realized, which avoided the traditional cell counting procedures. In this system, the CL emission of luminol-based system was served as the inner excitation light source, which simplified the instrument largely. In addition, with the aid of the sensitization of the CdTe QDs to the porous ZnO and the LSPR produced from GMSNs, the proposed biosensor showed a detection limit of 21 cells per mL and excellent selectivity. Our work had a further profound understanding about the expression of N-glycan on cell surface. In consideration of the abnormal expression of the N-glycan on the surface of cell with pathological changes, the proposed PEC biosensor opens a new promising platform for glycomics studies in clinical diagnostics and drug screening.

ASSOCIATED CONTENT

Supporting Information

Culture and treatment of cells, synthesis of the materials used in this work, characterizations of the ZnO, GQDs and CdTe, CL spectra of luminol-HRP-H_2O_2 system, fabrication of the PEC detection areas, electrophoresis analysis, optimization of the conditions, N-glycan expression. This material is available free of charge via the Internet at http://pubs.acs.org.

AUTHOR INFORMATION

Corresponding Author

*Tel: +86-531-82767161; Fax: +86-531-82765969;

*E-mail address: ujn.yujh@gmail.com

Notes

The authors declare no competing financial interest.

ACKNOWLEDGMENT

This work was financially supported by the National Natural Science Foundation of China (21575051, 21475052) and the Nature Science Foundation of Shandong Province, China (ZR2015JL006, ZR2014EMP010).

REFERENCES

(1) Zhao, W. W.; Zhang, L.; Xu, J. J.; Chen, H. Y. Cell Surface Carbohydrates Evaluation via a Photoelectrochemical Approach. *Chem. Commun.* **2012**, *48*, 9456-9458.

(2) Han, E.; Ding, L.; Qian, R.; Bao, L.; Ju, H. Sensitive Chemiluminescent Imaging for Chemoselective Analysis of Glycan Expression on Living Cells using a Multifunctional Nanoprobe. *Anal. Chem.* 2012, *84*, 1452-8

(3) Dennis, J. W.; Nabi, I. R.; Demetriou, M. Metabolism, Cell Surface Organization, and Disease. *Cell* **2009**, *139*, 1229-1241.

(4) Marino, K.; Bones, J.; Kattla, J. J.; Rudd, P. M. A Systematic Approach to Protein Glycosylation Analysis: A Path through the Maze. *Nat. Chem. Biol.* **2010**, *6*, 713-723.

(5) Zhang, X.; Teng, Y.; Fu, Y.; Xu, L.; Zhang, S.; He, B.; Wang, C.; Zhang, W. Lectin-Based Biosensor Strategy for Electrochemical Assay of Glycan

Expression on Living Cancer Cells. *Anal. Chem.* **2010**, *82*, 9455-9460.

(6) Xiao, H.; Tang, G. X.; Wu, R. Site-Specific Quantification of Surface N-Glycoproteins in Statin-Treated Liver Cells. *Anal. Chem.* **2016**, *88*, 3324-3332.

(7) Fuster, M. M.; Esko, J. D. The Sweet and Sour of Cancer: Glycans as Novel Therapeutic Targets. *Nat. Rev. Cancer* **2005**, *5*, 526-542.

(8) Wang, J. Z.; Grundke-Iqbal, I.; Iqbal, K. Glycosylation of Microtubule-Associated Protein Tau: An Abnormal Posttranslational Modification in Alzheimer's Dsease. *Nat. Med.* **1996**, *2*, 871-875.

(9) Christiansen, M. N.; Chik, J.; Lee, L.; Anugraham, M.; Abrahams, J. L.; Packer, N. H. Cell Surface Protein Glycosylation in Cancer. *Proteomics* **2014**, *14*, 525-546.

(10) Vigerust, D. Protein Glycosylation in Infectious Disease Pathobiology and Treatment. *Open Life Sci.*, **2011**, 6, 802-816.

(11) Kaneshiro, K.; Watanabe, M.; Terasawa, K.; Uchimura, H.; Fukuyama, Y.; Iwamoto, S.; Sato, T.-A.; Shimizu, K.; Tsujimoto, G.; Tanaka, K. Rapid Quantitative Profiling of N-Glycan by the Glycan-Labeling Method Using 3-Aminoquinoline/α-Cyano-4-hydroxycinnamic Acid *Anal. Chem.* **2012**, *84*, 7146-7151.

(12) Vanderschaeghe, D.; Szekrényes, Á.; Wenz, C.; Gassmann, M.; Naik, N.; Bynum, M.; Yin, H.; Delanghe, J.; Guttman, A.; Callewaert, N. High-Throughput Profiling of the Serum N-Glycome on Capillary Electrophoresis Microfluidics Systems: Toward Clinical Implementation of GlycoHepatoTest. *Anal. Chem.* **2010**, *82*, 7408-7415.

(13) Carneiro, M. G.; Koharudin, L. M. I.; Ban, D.; Sabo, T. M.; Trigo-Mourino, P.; Mazur, A.; Griesinger, C.; Gronenborn, A. M.; Lee, D. Sampling of Glycan-Bound Conformers by the Anti-HIV Lectin Oscillatoria Agardhii

Agglutinin in the Absence of Sugar. *Angew. Chem., Int. Ed.* **2015**, *54*, 6462-6465.

(14) Royle, L.; Campbell, M. P.; Radcliffe, C. M.; White, D. M.; Harvey, D. J.; Abrahams, J. L.; Kim, Y.-G.; Henry, G. W.; Shadick, N. A.; Weinblatt, M. E.; Lee, D. M.; Rudd, P. M.; Dwek, R. A. HPLC-ased Analysis of Serum N-glycans on a 96-well Plate Platform with Dedicated Database Software. *Anal. Biochem.* **2008**, *376*, 1-12.

(15) He, Y.; Li, J. H.; Liu, Y. Reusable and Dual-Potential Responses Electrogenerated Chemiluminescence Biosensor for Synchronously Cytosensing and Dynamic Cell Surface N-Glycan Evaluation. *Anal. Chem.* **2015,** *87***,** 9777-9785.

(16) Liu, H.; Li, X.; Crooks, R. M. Paper-Based SlipPAD for High-Throughput Chemical Sensing. *Anal. Chem.* **2013**, *85*, 4263-4267.

(17) Zhang, Y.; Li, L.; Zhang, L.; Ge, S.; Yan, M.; Yu, J. In-situ Synthesized Polypyrrole-cellulose Conductive networks for Potential-tunable Foldable Power Paper. *Nano Energy* **2017**, *31*, 174-182.

(18) Ge, S., Zhang, L., Zhang, Y., Lan, F., Yan, M., Yu, J., Nanomaterials Modified Cellulose Paper as a Platform for Biosensing Application. *Nanoscale*, **2017**, DOI: 10.1039/C6NR08846E.

(19) Credou, J.; Berthelot, T. Cellulose: from Biocompatible to Bioactive Material. *J. Mater. Chem. B* **2014**, *2*, 4767-4788.

(20) Yetisen, A. K.; Akram, M. S.; Lowe, C. R. Paper-based Microfluidic Point-of-care Diagnostic Devices. *Lab Chip* **2013**, *13*, 2210-2251.

(21) Bellani, S.; Ghadirzadeh, A.; Meda, L.; Savoini, A.; Tacca, A.; Marra, G.; Meira, R.; Morgado, J.; Di Fonzo, F.; Antognazza, M. R. Hybrid Organic/Inorganic Nanostructures for Highly Sensitive Photoelectrochemical Detection of Dissolved Oxygen in Aqueous Media. *Adv. Funct. Mater.* **2015**, *25*, 4531-4538.

(22) Tang, J.; Zhang, Y.; Kong, B.; Wang, Y.; Da, P.; Li, J.; Elzatahry, A. A.; Zhao, D.; Gong, X.; Zheng, G. Solar-Driven Photoelectrochemical Probing of Nanodot/Nanowire/Cell Interface. *Nano Lett.* **2014**, *14*, 2702-2708.

(23) Ma, W.; Han, D.; Zhou, M.; Sun, H.; Wang, L.; Dong, X.; Niu, L. Ultrathin g-C_3N_4/TiO_2 Composites as Photoelectrochemical Elements for the Real-Time Evaluation of Global Antioxidant Capacity. *Chem. Sci.* **2014**, *5*, 3946-3951.

(24) Zhang, X.; Xu, Y.; Yang, Y.; Jin, X.; Ye, S.; Zhang, S.; Jiang, L. A New Signal-On Photoelectrochemical Biosensor Based on a Graphene/Quantum-Dot Nanocomposite Amplified by the Dual-Quenched Effect of Bipyridinium Relay and AuNPs. *Chem. Eur. J.* **2012**, *18*, 16411-16418.

(25) Tang, J.; Wang, Y.; Li, J.; Da, P.; Geng, J.; Zheng, G. Sensitive Enzymatic Glucose Detection by TiO_2 Nanowire Photoelectrochemical Biosensors. *J. Mater. Chem. A* **2014**, *2*, 6153-6157.

(26) Li, C.; Wang, H.; Shen, J.; Tang, B. Cyclometalated Iridium Complex-Based Label-Free Photoelectrochemical Biosensor for DNA Detection by Hybridization Chain Reaction Amplification. *Anal. Chem.* **2015**, *87*, 4283-4291.

(27) Tu, W.; Wang, W.; Lei, J.; Deng, S.; Ju, H., Chemiluminescence excited photoelectrochemistry using graphene-quantum dots nanocomposite for biosensing. *Chem. Commun.* **2012**, *48*, 6535-6537.

(28) Abdolmohammad-Zadeh, H.; Rahimpour, E. Utilizing of Ag@AgCl@graphene oxide@Fe_3O_4 Nanocomposite as a Magnetic Plasmonic Nanophotocatalyst in Light-Initiated H_2O_2 Generation and Chemiluminescence Detection of Nitrite. *Talanta* **2015**, *144*, 769-777.

(29) Xu, K.; Sun, Y.; Li, W.; Xu, J.; Cao, B.; Jiang, Y.; Zheng, T.; Li, J.; Pan, D. Multiplex Chemiluminescent Immunoassay for Screening of Mycotoxins Using Photonic Crystal Microsphere Suspension Array. *Analyst* **2014**, *139*, 771-777.

(30) Iranifam, M.; Khabbaz Kharameh, M. Cupric Oxide Nanoparticles-enhanced Chemiluminescence Method for Measurement of β-lactam Antibiotics. *Luminescence* **2015**, *30*, 625-630.

(31) Khajvand, T.; Chaichi, M. J.; Colagar, A. H. Sensitive Assay of Hexythiazox Residue in Citrus Fruits Using Gold Nanoparticles-catalysed Luminol–H_2O_2 Chemiluminescence. *Food Chem.* **2015**, *173*, 514-520.

(32) Ge, Z. L.; Lin, M. H.; Wang, P.; Pei, H.; Yan, J.; Shi, J. Y.; Huang, Q.; He, D. N., Fan, C. H.; Zuo, X. L. Hybridization Chain Reaction Amplification of MicroRNA Detection with a Tetrahedral DNA Nanostructure-Based Electrochemical Biosensor. *Anal. Chem.* **2014,** *86***,** 2124-2130.

(33) Zhou, G. B.; Lin, M. H.; Song, P.; Chen, X. Q.; Chao, J.; Wang, L. H.; Huang, Q.; Huang, W.; Fan, C. H.; Zuo, X. L. Multivalent Capture and Detection of Cancer Cells with DNA Nanostructured Biosensors and Multibranched Hybridization Chain Reaction Amplification. *Anal. Chem.* **2014,** *86***,** 7843-7848.

(34) Zhang, Y.; Ge, L.; Li, M.; Yan, M.; Ge, S.; Yu, J.; Song, X.; Cao, B. Flexible Paper-based ZnO Nanorod Light-emitting Diodes Induced Multiplexed Photoelectrochemical Immunoassay. *Chem. Commun.* **2014**, *50*, 1417-1419.

(35) Hu, Z.; Li, J.; Li, C.; Zhao, S.; Li, N.; Wang, Y.; Wei, F.; Chen, L.; Huang, Y. Folic Acid-Conjugated Graphene-ZnO Nanohybrid for Targeting Photodynamic Therapy under Visible Light Irradiation. *J. Mater. Chem. B* **2013**, *1*, 5003-5013.

(36) Lan, F.; Sun, G.; Liang, L.; Ge, S.; Yan, M.; Yu, J. Microfluidic Paper-based Analytical Device for Photoelectrochemical Immunoassay with Multiplex Signal Amplification Using Multibranched Hybridization Chain Reaction and PdAu Enzyme Mimetics. *Biosens. Bioelectron.* **2016**, *79*, 416-422.

(37) Shi, Y.; Wang, J.; Wang, C.; Zhai, T. T.; Bao, W. J.; Xu, J. J.; Xia, X. H.; Chen, H. Y. Hot Electron of Au Nanorods Activates the Electrocatalysis of Hydrogen Evolution on MoS_2 Nanosheets. *J. Am. Chem. Soc.* **2015**, *137*, 7365-7370.

(38) Yan, Z.; Wang, Z.; Miao, Z.; Liu, Y. Dye-Sensitized and Localized Surface Plasmon Resonance Enhanced Visible-Light Photoelectrochemical Biosensors for Highly Sensitive Analysis of Protein Kinase Activity. *Anal. Chem.* **2016**, *88*, 922-929.

(39) Wu, K.; Rodríguez-Córdoba, W. E.; Yang, Y.; Lian, T. Plasmon-Induced Hot Electron Transfer from the Au Tip to CdS Rod in CdS-Au Nanoheterostructures. *Nano Lett.* **2013**, *13*, 5255-5263.

(40) Gomes Silva, C.; Juárez, R.; Marino, T.; Molinari, R.; García, H. Influence of Excitation Wavelength (UV or Visible Light) on the Photocatalytic Activity of Titania Containing Gold Nanoparticles for the Generation of Hydrogen or Oxygen from Water. *J. Am. Chem. Soc.* **2011**, *133*, 595-602.

(41) Hoggard, A.; Wang, L.-Y.; Ma, L.; Fang, Y.; You, G.; Olson, J.; Liu, Z.; Chang, W.-S.; Ajayan, P. M.; Link, S. Using the Plasmon Linewidth to Calculate the Time and Efficiency of Electron Transfer between Gold Nanorods and Graphene. *ACS Nano* **2013**, *7*, 11209-11217.

(42) Kong, B.; Tang, J.; Selomulya, C.; Li, W.; Wei, J.; Fang, Y.; Wang, Y.; Zheng, G.; Zhao, D. Oriented Mesoporous Nanopyramids as Versatile Plasmon-Enhanced Interfaces. *J. Am. Chem. Soc.* **2014**, *136*, 6822-6825.

(43) Zhao, W.-W.; Wang, J.; Xu, J.-J.; Chen, H.-Y. Energy Transfer between CdS Quantum Dots and Au Nanoparticles in Photoelectrochemical Detection. *Chem. Commun.* **2011**, *47*, 10990-10992.

(44) Baker, S. N.; Baker, G. A. Luminescent Carbon Nanodots: Emergent Nanolights. *Angew. Chem., Int. Ed.* **2010**, *49*, 6726-6744.

(45) Zhuo, S.; Shao, M.; Lee, S.-T. Upconversion and Downconversion Fluorescent Graphene Quantum Dots: Ultrasonic Preparation and Photocatalysis. *ACS Nano* **2012**, *6*, 1059-1064.

(46) Peng, J.; Gao, W.; Gupta, B. K.; Liu, Z.; Romero-Aburto, R.; Ge, L.; Song, L.; Alemany, L. B.; Zhan, X.; Gao, G.; Vithayathil, S. A.; Kaipparettu, B. A.; Marti, A. A.; Hayashi, T.; Zhu, J.-J.; Ajayan, P. M. Graphene Quantum Dots Derived from Carbon Fibers. *Nano Lett.* **2012**, *12*, 844-849.

(47) Zhang, G.; Shen, X.; Yang, Y. Facile Synthesis of Monodisperse Porous ZnO Spheres by a Soluble Starch-Assisted Method and Their Photocatalytic Activity. *J. Phys. Chem. C* **2011**, *115*, 7145-7152.

(48) Guo, C. X.; Dong, Y.; Yang, H. B.; Li, C. M. Graphene Quantum Dots as a Green Sensitizer to Functionalize ZnO Nanowire Arrays on F-Doped SnO_2Glass for Enhanced Photoelectrochemical Water Splitting. *Adv. Energy Mater.* **2013**, *3*, 997-1003.

(49) Fan, G. C.; Han, L.; Zhang, J. R.; Zhu, J. J. Enhanced Photoelectrochemical Strategy for Ultrasensitive DNA Detection Based on Two Different Sizes of CdTe Quantum Dots Cosensitized TiO_2/CdS:Mn Hybrid Structure. *Anal. Chem.* **2014**, *86*, 10877-10884.

(50) Liu, B.; Zhang, B.; Cui, Y.; Chen, H.; Gao, Z.; Tang, D. Multifunctional Gold-Silica Nanostructures for Ultrasensitive Electrochemical Immunoassay of Streptomycin Residues. *ACS Appl. Mater. Interfaces* **2011**, *3*, 4668-4676.

(51) Yu, W. W.; Qu, L.; Guo, W.; Peng, X. Experimental Determination of the Extinction Coefficient of CdTe, CdSe, and CdS Nanocrystals. *Chem. Mater.* **2003**, *15*, 2854-2860.

(52) Chen, X.; Wang, Y.; Zhou, J.; Yan, W.; Li, X.; Zhu, J.-J. Electrochemical Impedance Immunosensor Based on Three-Dimensionally Ordered Macroporous Gold Film. *Anal. Chem.* **2008**, *80*, 2133-2140.

(53) Chen, X.; Wang, Y.; Zhang, Y.; Chen, Z.; Liu, Y.; Li, Z.; Li, J. Sensitive Electrochemical Aptamer Biosensor for Dynamic Cell Surface N-Glycan Evaluation Featuring Multivalent Recognition and Signal Amplification on a

Dendrimer–Graphene Electrode Interface. *Anal. Chem.* **2014**, *86*, 4278-4286.

(54) Chen, X.; He, Y.; Zhang, Y.; Liu, M.; Liu, Y.; Li, J. Ultrasensitive Detection of Cancer Cells and Glycan Expression Profiling Based on a Multivalent Recognition and Alkaline Phosphatase-Responsive Electrogenerated Chemiluminescence Biosensor. *Nanoscale* **2014**, *6*, 11196-11203.

(55) Liu, J.; Zhou, H.; Xu, J. J.; Chen, H. Y. An Effective DNA-based Electrochemical Switch for Reagentless Detection of Living Cells. *Chem. Commun.* **2011**, *47*, 4388-4390.

(56) Zhao, J.; Zhang, L.; Chen, C.; Jiang, J.; Yu, R. A Novel Sensing Platform using Aptamer and RNA Polymerase-based Amplification for Detection of Cancer Cells. *Anal. Chim. Acta* **2012**, *745*, 106-111.

(57) Han, E.; Ding, L.; Qian, R.; Bao, L.; Ju, H. Sensitive Chemiluminescent Imaging for Chemoselective Analysis of Glycan Expression on Living Cells using a Multifunctional Nanoprobe. *Anal. Chem*. **2012**, *84*, 1452-1458.

(58) Chen, X.; He, Y.; Zhang, Y.; Liu, M.; Liu, Y.; Li, J. Ultrasensitive Detection of Cancer Cells and Glycan Expression Profiling Based on a Multivalent Recognition and Alkaline Phosphatase-responsive Electrogenerated Chemiluminescence Biosensor. *Nanoscale* **2014**, *6*, 11196-11203.

(59) Liang, L.; Lan, F.; Li, L.; Ge, S.; Yu, J.; Ren, N.; Liu, H.; Yan, M. Paper Analytical Devices for Dynamic Evaluation of Cell Surface N-glycan Expression via a Bimodal Biosensor Based on Multibranched Hybridization Chain Reaction Amplification. *Biosens. Bioelectron.* **2016**, *86*, 756-763.

(60) Qian, Z.; Bai, H. J.; Wang, G. L.; Xu, J. J.; Chen, H. Y. A Photoelectrochemical Sensor Based on CdS-polyamidoamine Nano-composite Film for Cell Capture and Detection. *Biosens. Bioelectron.* **2010**, *25* , 2045-2050.

(61) Zhao, W. W.; Zhang, L.; Xu, J. J.; Chen, H. Y. Cell Surface Carbohydrates

Evaluation via a Photoelectrochemical Approach. *Chem. Commun.* **2012**, *48*, 9456-9458.

(62) Su, M.; Ge, L.; Kong, Q.; Zheng, X.; Ge, S.; Li, N.; Yu, J.; Yan, M.Cyto-sensing in Electrochemical Lab-on-paper Cyto-device for in-situ Evaluation of Multi-glycan Expressions on Cancer Cells. *Biosens. Bioelectron.* **2015**, *63*, 232-239.

(63) Chen, Z.; Liu, Y.; Wang, Y.; Zhao, X.; Li, J. Dynamic Evalua1ption of Cell Surface N-Glycan Expression via an Electrogenerated Chemiluminescence Biosensor Based on Concanavalin A-integrating Gold-nanoparticle-modified $Ru(bpy)_3^{(2+)}$-doped Silica Nanoprobe. *Anal. Chem.* **2013**, *85*, 4431-4438.

Table of Contents Graphic